r_0; however, a reasonable estimate of $r_0 \approx 100\ \mu$ gives a net Raman gain of 2.1 Np at the maximum input power of 2 kW. This clearly allows us to obtain Raman laser oscillation at $B = 50$ kG. Since the spontaneous spin-flip Raman scattering efficiency, $S/ld\Omega$, drops very rapidly as the magnetic field is reduced from 55 to 30 kG (as seen in Fig. 24 of Ref. 3) it is reasonable that in the present geometry the Raman laser does not work below $B \approx 45$ kG. Above $B \approx 50$-60 kG, the Raman scattering efficiency goes up by a factor of 2 as B is increased to 100 kG, but the free-carrier absorption goes up by a factor of 3-4, and the stimulated Raman power output at $B = 100$ kG drops by a factor of 20 from its maximum value at $B = 58$ kG. Above $B = 100$ kG stimulated Raman scattering is not obtained which is ascribed to the high free carrier absorption. A different sample geometry may remove some of these restrictions.

In conclusion, we have demonstrated a tunable stimulated spin-flip Raman scattering process arising from conduction electrons in InSb. The Raman laser output of ~1-W peak is tunable from ~11.7 to 13.0 μ by changing the magnetic field from 48 to 100 kG. It may be possible to improve the present conversion efficiency of $\sim 5 \times 10^{-4}$ by increasing the pump power and by shortening the spin relaxation time for the electrons in InSb. The extremely narrow linewidth of 0.05 cm^{-1} together with the high peak and average power makes the spin-flip Raman laser ideally suitable for high-resolution spectroscopy and as a local oscillator in communication systems. Higher magnetic fields together with an improved sample geometry, such as collinear pump and Raman-scattered light, and high-reflectivity coatings on the InSb sample will both increase the tunability of the spin-flip Raman laser and lower its threshold leading to higher conversion efficiencies.

The authors thank R. J. Kerl for excellent technical assistance, A. L. Albert for skillful polishing of the InSb crystals, and Dr. R. E. Slusher and Dr. P. A. Wolff for helpful comments on the manuscript.

---

[1] Y. Yafet, Phys. Rev. 152, 858 (1966).

[2] R. E. Slusher, C. K. N. Patel, and P. A. Fleury, Phys. Rev. Letters 18, 77 (1967).

[3] C. K. N. Patel, Modern Optics (Polytechnic Press, Brooklyn, N. Y., 1967) Vol. XVII, pp. 19-51.

[4] C. K. N. Patel and R. E. Slusher, Phys. Rev. 167, 413 (1968), and 177, 1200 (1969).

[5] P. A. Wolff, J. Quantum Electron. 2, 659 (1966), and Phys. Rev. Letters 16, 225 (1966).

[6] W. D. Johnston, Jr., and I. P. Kaminow, Phys. Rev. 168, 1045 (1968), and 178, 1528(E) (1969), and references cited herein; W. D. Johnston, Jr., I. P. Kaminow and J. G. Bergman, Jr., Appl. Phys. Letters 13, 190 (1968).

[7] V. P. Makarov, Zh. Eksperim. i. Teor. Fiz. Pis'ma Redakt. 55, 704 (1968) [JETP Letters 28, 366 (1969)]; B. S. Wherrett and P. G. Harper, Phys. Rev. 183, 692 (1969).

[8] C. K. N. Patel and K. H. Yang, to be published.

[9] C. K. N. Patel and E. D. Shaw, to be published.

[10] C. K. N. Patel and R. E. Slusher, Phys. Rev. Letters 19, 1019 (1967).

[11] P. A. Wolff, private communication.

LUMINESCENCE SPECTRA OF EUROPIUM CHALCOGENIDES: EuO, EuS, and EuSe†

R. Tsu and L. Esaki
IBM Thomas J. Watson Research Center, Yorktown Heights, New York

(Received 20 January 1970)

Electron-beam—excited luminescence spectra for EuO, EuS, and EuSe show a series of broad and sharp peaks in the energy range from 1 to 4 eV at temperatures between 12 and 300°K. The low-energy broad peaks, corresponding to $4f^7$-$4f^6 5d$ transition, exhibit a redshift, having energies lower than the optical absorption peaks due to a Franck-Condon-like effect. At higher energies, we have observed a series of sharp peaks arising from intra-atomic transitions within the $4f$ configuration in the Eu ions.

In the luminescence spectra of the europium chalcogenides, EuO, EuS, and EuSe, excited by an electron beam, we have found striking structure consisting of a series of broad and sharp peaks, in the photon energy range of 1 to 4 eV, and at temperatures between 12 and 300°K. An electron beam of 10–20 keV and $(1-3)\times 10^{-4}$ $\mathrm{A/cm^2}$, modulated at low frequencies, is focused within a spot of size a few square millimeters on the cleaved surface of nominally pure, single crystals mounted on a cold finger. The emitted luminescence is dispersed by a $\mathrm{CaF_2}$ prism spectrometer, and detected by either S-1 or S-13 photomultiplier dependent upon the photon energy.

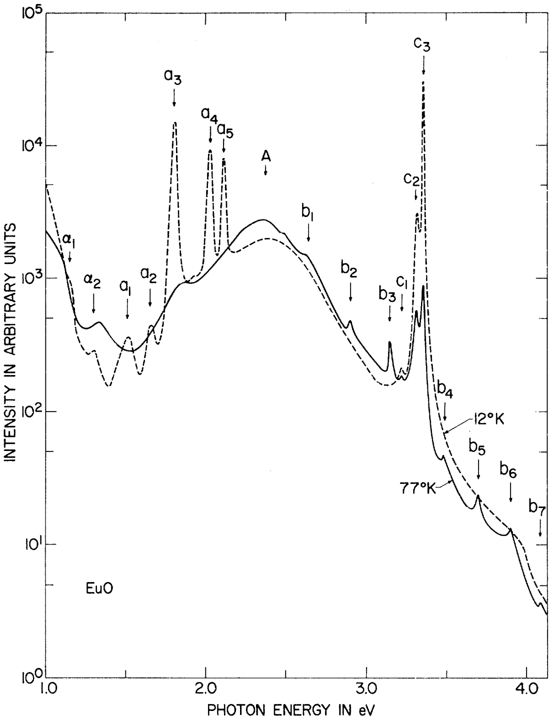

FIG. 1. Luminescence intensity versus photon energy for EuO at 12 and 77°K.

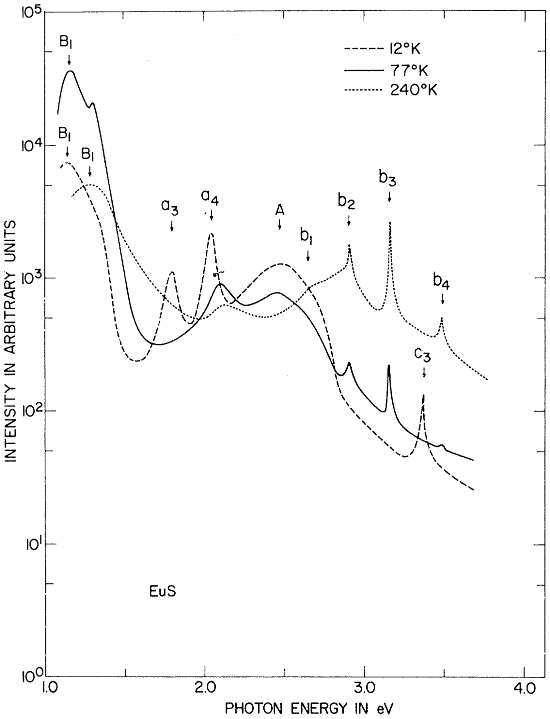

FIG. 2. Luminescence intensity versus photon energy for EuS at 12, 77, and 240°K.

Crystals doped with Gd or containing excess Eu show the same general pattern in the spectra, though having less prominent structure.

In Figs. 1-3, we illustrate the typical semilog plot of the luminescence intensity as a function of photon energy for EuO, EuS, and EuSe, respectively. The same arbitrary intensity scale is used throughout these three figures, where dashed, solid, and dotted lines correspond to 12, 77, and 240°K, respectively. All curves seem to be characterized by the following features: There are high-intensity broad peaks designated by B_i at low energies (except for EuO, whose corresponding peaks apparently are less than 1 eV), and at higher energies, starting at 1.5 eV, there are three series of sharp peaks designated by a_i, b_i, and c_i, apparently common to all crystals. Table I summarizes these experimental results together with reported optical absorption peaks[1,2] in the top row and the known atomic transition energies[3,4] within the $4f$ configuration of Eu ions in the last column.

The low-energy peak B_1, which exhibits a redshift[5,6] and an increasing intensity with decrease in temperature (except below the Curie temperature), is believed to be the transition between the $4f^7(^8S_{7/2})$ ground state and a magnetic exciton state belonging to $4f^6(^7F_J)5d(t_{2g})$ with $J=0, 1, \cdots, 6$. As seen in Table I, these energies are considerably lower than the optical absorption

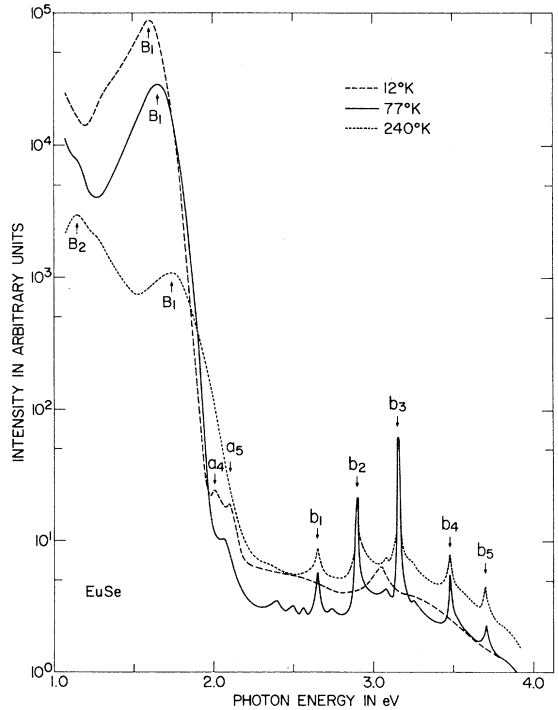

FIG. 3. Luminescence intensity versus photon energy for EuSe at 12, 77, and 240°K.

Table I. Observed peak energies in eV at 12, 77, and 240°K with their corresponding atomic transition energies in the last column and reported optical absorption peaks in the top row.

	EuO		EuS			EuSe			transitions involved	
optical abs. peak at 300°K	2.1		2.4			2.6 eV				
	12	77°K	12	77	240°K	12	77	240°K		
B_2	-	-	-	-	-	< 1	< 1	1.15	impurities ?	
B_1	< 1		1.14	1.17	1.28	1.60	1.66	1.74	$4f^7 - 4f^6 5d$	
α_1	1.15	-	-	-	-	-	-	-	$4f^7 - 4f^6(^7F_5)$ 5d ?	
α_2	1.30	-	-	-	-	-	-	-	$4f^7 - 4f^6(^7F_6)$ 5d ?	
a_1	1.52	-	-	-	-	-	-	-	$^5D_0 - ^7F_6$	1.53
a_2	1.66	-	-	-	-	-	-	-	$^5D_0 - ^7F_5$	1.66
a_3	1.81	-	1.81	-	-	-	-	-	$^5D_0 - ^7F_4$	1.80
a_4	2.03	-	2.03	-	-	2.02	-	-	$^5D_0 - ^7F_2$ $^5D_1 - ^7F_4$	2.01 2.02
a_5	2.12	-	-	-	-	2.11	-	-	$^5D_0 - ^7F_1$ $^5D_1 - ^7F_3$	2.10 2.13
A	2.40	2.35	2.48	2.45	-	-	-	-	$^5D_1 - ^7F_0$ etc.	2.36 etc.
b_1	-	2.65	-	-	-	-	2.65	2.65		
b_2	-	2.90	-	2.90	2.91	-	2.90	2.90		
b_3	-	3.15	-	3.16	3.17	-	3.16	3.16		
b_4	-	3.48	-	3.48	3.48	-	3.48	3.48		
b_5	-	3.70	-	-	-	-	3.71	3.70		
b_6	-	3.90	-	-	-	-	-	-		
b_7	-	4.08	-	-	-	-	-	-		
c_1	3.22	3.22	-	-	-	-	-	-	$^6P_{7/2} - ^8S_{7/2}$	3.24 (3.98x0.815)
c_2	3.32	3.31	-	-	-	-	-	-	$^6P_{5/2} - ^8S_{7/2}$	3.30 (4.05x0.815)
c_3	3.36	3.36	3.36	-	-	-	-	-	$^6P_{3/2} - ^8S_{7/2}$	3.36 (4.12x0.815)

peaks, which may be explained by invoking a Franck-Condon-like effect proposed by Kasuya and Yanase.[7] Indeed, in the case of EuSe, the B_1 peak agrees quite well with a peak in the photoluminescence observed by Busch and Wachter,[8] whereas the B_2 peak probably has a different origin, such as impurities. In EuS, we have noticed that the B_1 peak markedly decreases in intensity at the onset of the ferromagnetic order around 17°K, which is also reminiscent of the above-mentioned photoluminescence result in EuSe. In EuO, although only a portion of the slope of the peak is seen in Fig. 1, we have observed two bumps α_1 and α_2 at 12°K, which could be attributed to fine structure of the magnetic exciton states. In this context, the α_1 and α_2 may be assigned to $4f^6(^7F_5)5d(t_{2g})$ and $4f^6(^7F_6)5d(t_{2g})$, respectively, as listed in Table I.

On the other hand, the three series of peaks at higher energies, a_i, b_i, and c_i, may be ascribed to intra-atomic transitions within the $4f$ electron configuration of Eu ions. Particularly, the energies of the a_i peaks agree beyond any doubt with the atomic energy levels of Eu^{3+} in $LaCl_3$ measured by DeShazer and Dieke,[3] as listed in the last column of Table I. A broad peak A in EuO and EuS is probably composed of a number of transition lines whose energies are very close in these ^5D-to-^7F transition series. At further higher energies, one sees the c_i peaks, particularly strong in EuO. Taking the results of Gd^{3+} energy levels in $LaCl_3$ by Piksis, Dieke, and Crosswhite,[4] and scaling these values by a factor of 0.815,[2] one finds that c_1, c_2, and c_3 are in good agreement with the scaled-down values, as seen in Table I. Thus, we tentatively assign these to three ^6P-to-^8S transitions in Eu^{2+}. The c_3 peak at 3.36 eV, believed to correspond to the $^6P_{3/2}$-$^8S_{7/2}$ transition, is most pronounced among the three and shows surprisingly high intensity at 12°K for EuO. The observed linewidth is only 15 meV which seems comparable with the crystal-field splitting of the ground state, considering that the $J=\frac{3}{2}$ state is a singlet, while the $J=\frac{7}{2}$ state is a triplet, in a rocksalt-type crystal.

Next we will consider the b_i series which show quite unusual properties. They start at 2.65 eV and the most intense peak is at 3.15-3.17 eV in all crystals studied. It should be pointed out that all of them disappear completely at low temperatures. The results for EuO are particularly informative. They suddenly disappear at the onset of the ferromagnetic ordering around 70°K. More precisely, its intensity, which is fairly constant at higher temperatures, begins to decrease at 80°K and shows 60 ~ 70% at 70°K and only less than 10% of the original value at 60°K. We believe that, whatever the origin is, the spin ordering or the spin wave has profound influences on these emissions. We would like to point out further that this temperature dependence is entirely opposite to that of the other peaks, most of which are only seen at low temperatures. For instance, the height of the 3.36-eV peak at 77°K is only 5% of that at 12°K.

Now, let us look into the scattering, ionization, and excitation processes by incident electrons in europium chalcogenide crystals as well as Eu ions alone. In our experimental condition, high incident-electron energies obviously give rise to a number of high-energy excitations. These excited electrons, however, relax very rapidly to the bottom of each band and further will be trapped to localized impurity levels or excitonic states. The time constant in these processes is certainly dependent upon the capture cross section, the relaxation time of the electron-phonon interaction, etc. Nevertheless, the easiest excitation will be that of transferring one of the seven $4f$ electrons to the $5d(t_{2g})$ state. In this case, the excitation of the Eu^{2+} ground state $4f^7(^8S_{7/2})$ results in forming a magnetic exciton state involving an electron state $5d(t_{2g})$ and a holelike state $4f^6(^7F_J)$. The recombination of this excitonic state is believed to give rise to the broad B_1 peak which shows high luminescence intensity in our measurements and was observed even in the photoluminescence measurements.[8] The width of this peak is primarily due to the spread of seven ^7F_J states, which is known to be 0.6 eV. If, however, an exchange scattering accompanied by a spin flip is assumed to be allowed in our electron-beam excitation, we will see further variety of excitations. It is now possible to excite the above-mentioned ^7F_J states to ^5D_J states in the same $4f^6$ configuration. It is also possible to excite the Eu^{2+} ground state directly to ^6P_J states in the same $4f^7$ configuration. Preliminary measurements on luminescence intensity as a function of electron beam current indicate that the c_3 peak height is proportional to the square of the beam current, whereas the broad peak A has a linear dependence. Clearly, these processes are not simple. Nevertheless, from consideration of the energy values, we postulate that these transitions ^7F_J-^5D_J and $^8S_{7/2}$-^6P_J give rise to the a_i and c_i series, respectively. Furthermore, since these transitions occur without change in the $4f$ electron configuration, the observed lines are essentially atomic because the crystal field has little effect on the $4f$ electron energy levels. With measurements extended up to 5 eV photon energy, we have found no evidence of luminescence which may be identifiable as due to the $5d(e_g)$ state,[9] or due to other s or p bands.[10]

We have demonstrated that this approach provides significant additional information toward an understanding of the electronic structure in the europium chalcogenides. The technique is relatively simple and, particularly, advantageous from an experimental viewpoint because of less precaution required for surface preparation. Some of the observed phenomena such as the unusual properties of the b_i series, the dependence of the intensity upon the beam current, etc., remain to be explained. We believe that application of a magnetic field or studies of photon polarization possibly would help to clarify the situation in the future.

We are most grateful to T. Kasuya and other staff members of our magnetic materials group for the many helpful discussions, F. Holtzberg and M. W. Shafer for supplying the single crystals, and T. Hajos for his assistance on the experiments.

---

†Research sponsored in part by the Army Research Office–Durham, under Contract No. DAHCO4-69-0069.

[1] M. J. Freiser, F. Holtzberg, S. Methfessel, G. D. Pettit, M. W. Shafer, and J. C. Suits, Helv. Physica Acta. 41, 832 (1968).

[2] A comprehensive review on these materials was given by S. Methfessel and D. C. Mattis, in *Handbuch der Physik*, edited by S. Flügge (Springer-Verlag, Berlin, Germany, 1968), Vol. 18, Pt.1, pp. 389-562.

[3] L. G. DeShazer and G. H. Dieke, J. Chem. Phys. 38, 2190 (1962).

[4] A. H. Piksis, G. H. Dieke, and H. M. Crosswhite, J. Chem. Phys. 47, 5083 (1967).

[5] G. Busch, P. Junod, and P. Wachter, Phys. Letters 12, 11 (1964).

[6] B. E. Argyle, J. C. Suits, and M. J. Freiser, Phys. Rev. Letters 15, 822 (1965).

[7] T. Kasuya and A. Yanese, Rev. Mod. Phys. 40, 684 (1968).

[8] G. Busch and P. Wachter, Phys. Letters 20, 617 (1966).

[9] J. Feinleib, W. J. Scouler, J. O. Dimmock, J. Hanus, T. B. Read, and C. R. Pidgeon, Phys. Rev. Letters 22, 1385 (1969); J. O. Dimmock, in Proceedings of Symposium on Magnetic Semiconductors, Yorktown Heights, New York, 13-14 November 1969 (to be published); C. R. Pidgeon, J. Feinleib, and W. J. Scouler, *ibid.*

[10] S. J. Cho, Phys. Rev. 157, 632 (1967).

TRAPPING OF POSITRONS BY DISLOCATIONS IN ALUMINUM

P. Hautojärvi, A. Tamminen, and P. Jauho
Department of Technical Physics, Technical University of Helsinki, Otaniemi, Finland

(Received 19 January 1970)

Positron lifetime measurements have been performed in plastically deformed aluminum single crystals. Evidence of a second nonspurious lifetime component has been observed. The results are interpreted as the trapping of positrons by dislocations. The lifetimes are found to be 172 psec in the perfect crystal and 228 psec in a dislocation. The escape probability of trapped positrons is estimated to be zero.

Recently, attention has been paid to positron annihilation in deformed metals. The experimental results, which indicate the narrowing of the 2γ angular correlation[1] and the increase of the positron mean lifetime,[2,3] can be understood by assuming an attractive interaction between positrons and defects. This Letter describes positron lifetime measurements in plastically deformed aluminum. The results are discussed in terms of a trapping model, which has previously been applied successfully to vacancies in alkali halides[4] and metals.[5]

It is assumed in the trapping model that positrons, after having slowed down, annihilate in the perfect crystal with a rate λ_c. They are trapped by defects at a rate κ which is assumed to be proportional to the defect density. Denoting the annihilation rate of trapped positrons in defects by λ_d and the escape probability from a defect by δ, then, with the condition that no positrons are initially trapped, the number of positrons left at time t is given by[4,6]

$$\frac{n(t)}{n(0)}=\frac{\lambda_c-\Lambda_2}{\Lambda_1-\Lambda_2}e^{-\Lambda_1 t}+\frac{\Lambda_1-\lambda_c}{\Lambda_1-\Lambda_2}e^{-\Lambda_2 t}. \quad (1)$$

The decay constants Λ_1 and Λ_2 are obtained as the roots of the equation

$$\Lambda^2-(\lambda_c+\lambda_d+\kappa+\delta)\Lambda+(\lambda_c+\kappa)(\lambda_d+\delta)-\kappa\delta=0. \quad (2)$$

The special case with no escape ($\delta=0$) gives

$$\Lambda_1=\lambda_c+\kappa,$$
$$\Lambda_2=\lambda_d. \quad (3)$$

In a perfect crystal there is only the first component. When the defect density increases, the intensity and lifetime of the first component decrease until the second component dominates.

The aluminum samples were spark-cut from one large single crystal of 99.999% purity. They were electrolytically polished, annealed for 10 h at 600°C in an argon atmosphere, deformed, and polished again just before the lifetime measurements. The crystals were deformed by compression until the desired thickness reduction was achieved. The ^{22}Na source was prepared by sealing 3 μCi of evaporated ^{22}NaHCO$_3$ solution in a gold-covered Al foil of 1.5 mg/cm^2 thickness. The source was sandwiched between two identically deformed crystals. The lifetime measurements were performed with a fast-slow coincidence system with 1-in. × 1-in. Naton 136 scintillators and XP 1021 photomultipliers. The time resolution in positron measurements was 290 psec (full width at half-maximum). Each sample was counted for 2×20 h and about 7×10^5 coincidences were accumulated during this time.

The experimental lifetime spectra were first analyzed conventionally by using a two-exponential fit with a constant chance-coincidence back-